BOLLETTINO DI GEOFISICA TEORICA ED APPLICATA VOL. 38, N. 1-2 - MARCH-JUNE 1997

Horizontal electric dipole over inhomogeneous earth model having linear variation of conductivity with depth

N. P. SINGH and T. LAL

Department of Geophysics, Banaras Hindu University, Varanasi, India

(Received on August 10, 1994; accepted on August 16, 1995)

Abstract. The behaviour of the electromagnetic (em) field response of a horizontal electric dipole placed over the surface of a vertically inhomogeneous earth model having linear variation of conductivity with depth is studied. The problem is solved for a multi-layer earth model with an intermediate inhomogeneous layer, and numerical results are obtained for these three-layer earth models with the intermediate transitional layer possessing the linear variation of conductivity with depth. The effect of variation of transition layer thickness and conductivity contrast between the top and the bottom layers are presented in the form of the absolute-amplitude ratio of the em field components expressed as a function of numerical distance. Analysis shows the characteristic dependence of the em field response on conductivity inhomogeneity.

1. Introduction

Study of the em response over inhomogeneous earth models has been carried out by a number of researchers. Mallick and Roy (1971) derived the analytical solutions for the em field components of a vertical magnetic dipole placed over an inhomogeneous earth model having linear variation of conductivity with depth, while Abramovici and Chlamtac (1978) presented the numerical results for the em field response over such models. Further, Chlamtac and Abramovici (1981) presented the computational results for the em field response over inhomogeneous earth models due to a horizontal electric dipole, considering linear variation of conductivity with depth. Singh and Lal (1995) derived the analytical and numerical solutions for the em field response of a horizontal magnetic dipole placed over inhomogeneous earth models having exponential variation of conductivity with depth.

In the present paper, the problem of calculating the em field response of a horizontal electric dipole placed over the surface of an inhomogeneous earth model possessing linear variation of conductivity with depth, addressed by Chlamtac and Abramovici (1981) has been generalised to

Corresponding author: Prof. T. Lal; Department of Geophysics, Banaras Hindu University, Varanasi - 221005, India

© *1997 Osservatorio Geofisico Sperimentale*

a multi-layer earth model. The analytical and numerical solutions have been obtained for the three-layer earth models with the intermediate layer having the linear variation of conductivity with depth. Analytical solutions are obtained in terms of integral equations, whereas Chlamtac and Abramovici (1981) presented them in differential equation form. In contrast to the Runge-Kutta method of computation used by Chlamtac and Abramovici, we applied the linear digital filtering algorithm ZHANKS proposed by Anderson (1979), which is claimed to be rapid and accurate, for the computation of the em response. The accuracy of the algorithm compares favorably with single-precision numerical quadrature methods for well-behaved infinite-integrals containing Bessel functions of order 0 and 1.

2. Formulation and solution of the problem

The geometry of the multi-layer earth model under investigation is shown in Fig. 1. The earth model comprises a sequence of N layers, of which (N-1) layers are homogeneous and the *j*-th is inhomogeneous. The cartesian coordinate system (x, y, z) with its z-axis directed vertically upward is used. The cylindrical coordinate system (ρ, ϕ, z) is also used frequently in many places. A diagram showing the relation between these two coordinate systems is shown in the inset of Fig. 1. A horizontal electric dipole, carrying a low-frequency alternating current and oriented along the x-axis parallel to the surface, is placed at a height h above the model.

Let σ_j, μ_j, h_j (j=1, 2, ..., N) be the conductivities, permeabilities and depths to the lower boundaries of the layers. The conductivity and permeability of the free space are taken to be σ_o and μ_o respectively. Further, since the magnetic permeability value for the rock formations in general equals the free space value, it is assumed that for all the layers $\mu_j = \mu_o$ (j=1, 2, ..., N).

The conductivity σ_j in the j-th inhomogeneous layer, which acts as a transition zone, is assumed to vary in accordance with the linear variation with depth defined by the relation

$$\sigma_j(z) = \sigma_{j-1}\left[1 + \alpha_1\left(z + h_{j-1}\right)\right], \tag{1}$$

where α_1 is the constant dependent upon the model parameters.

Here the conductivity of the (j-1)-th layer gradually merges with that of the (j+1)-th layer through the j-th transition layer, so that $\sigma_j(z)=\sigma_{j-1}$ at $z=-h_{j-1}$, and $\sigma_j(z)=\sigma_{j+1}$ at $z=-h_j$.

The radiation constant γ_0 in the air, and γ_1, γ_2, ... γ_{j-1}, γ_{j+1} ... γ_N in the homogeneous layers, assume constant values, while $\gamma_j(z)$ in the transition layer follows the linear variation with depth in correspondence to the conductivity variation. Therefore, in terms of radiation constants, the above relations can be expressed as

$$\begin{aligned}\gamma_j^2(z) &= \gamma_{j-1}^2\left[1 + \alpha_1\left(z + h_{j-1}\right)\right] \\ &= \begin{cases}\gamma_{j-1}^2 & , \text{ at } z = -h_{j-1} \\ \gamma_{j+1}^2 & , \text{ at } z = -h_j\end{cases}\end{aligned} \tag{2}$$

where

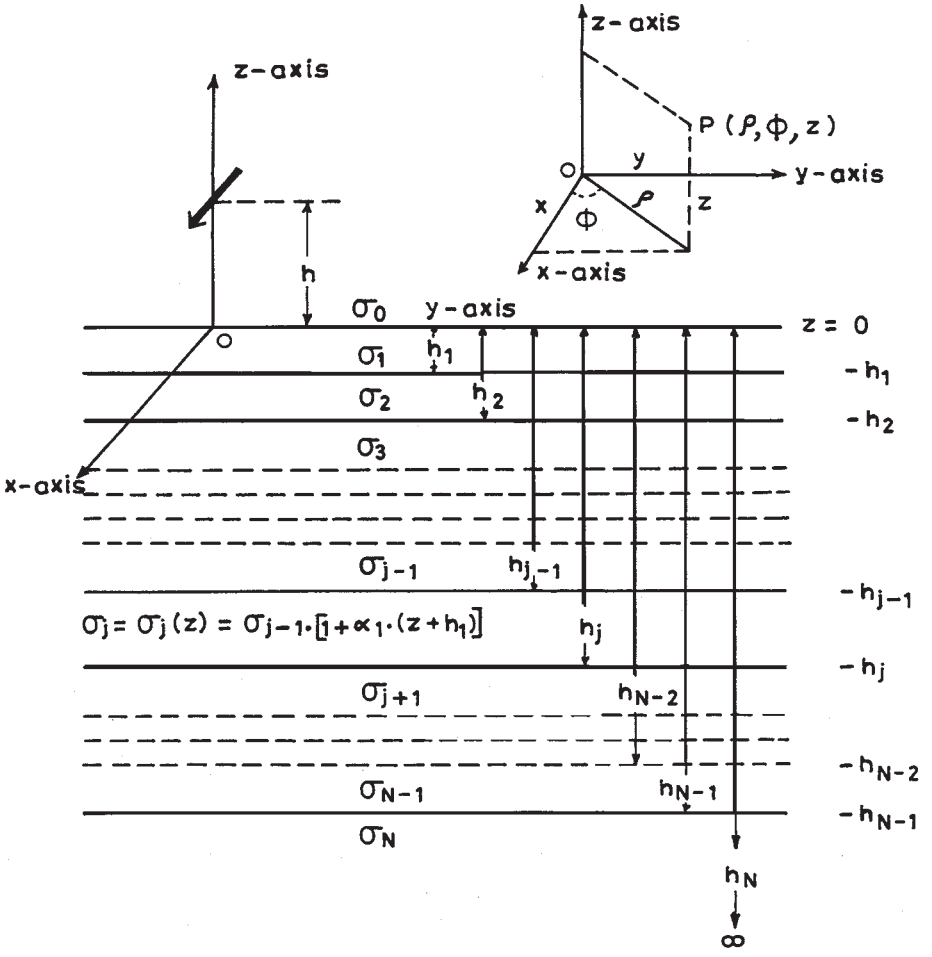

Fig. 1 - Geometry of the earth model under investigation.

$$\alpha_1 = \frac{1}{h_{j-1} - h_j}\left[\left(\frac{\gamma_{j+1}^2}{\gamma_{j-1}^2}\right)^2 - 1\right].$$

As the frequency of the current is low, the displacement currents in all the conductive media may be neglected. The harmonic time factor $e^{i\omega t}$ is implied.

Let *ds* be the length of the horizontal electric dipole, and *I* the low frequency alternating current flowing in the dipole. The primary Hertz vector potential (π_p), which has only an *x*-component, is given by

$$\pi = P\frac{e^{-\gamma_0 r}}{r}, \tag{3}$$

where

$$P = \frac{i\omega\mu_0 I\, ds}{4\pi\gamma_0^2},$$

$$\gamma_0^2 = -\xi_0 \mu_0 \omega^2,$$

and

$$r = \sqrt{\rho^2 + |(z-h)|^2}.$$

Using the Fourier-Bessel transform pair, the primary Hertz vector in the air can be expressed as

$$\pi = P\frac{e^{-\gamma_0 r}}{r} = P\int_0^\infty \frac{\lambda}{n_0} e^{\pm n_0|z-h|} J_0(\lambda\rho)\, d\lambda, \tag{4}$$

where λ is the separation constant and $n_0 = \sqrt{\lambda^2 + \gamma_0^2}$.

Since the dipole is oriented along the *x*-axis, the primary electric field is symmetrical about the *x*-*z* plane. While the primary potential has only an *x*-component, we need to employ two components for the secondary potentials. In general, therefore, we may write

$$\Pi = \mathbf{i}\,\pi_x + \mathbf{k}\,\pi_z \tag{5}$$

$$\pi_y = 0$$

wher **i** and **k** are unit vectors.

The harmonic electric and magnetic vector fields **E** and **H** are related to the Hertz vector (**Π**) by the relations

$$\mathbf{E} = \nabla\nabla\bullet\Pi - \gamma^2\,\Pi \tag{6}$$

$$\mathbf{H} = (\sigma + i\omega\xi)\nabla\times\Pi \tag{7}$$

The components of the fields can be written directly (Ward, 1967) as

$$\begin{aligned}
E_x &= -i\omega\mu(\sigma+i\omega\varepsilon)\pi_x + \frac{\partial}{\partial x}\left(\frac{\partial\pi_x}{\partial x} + \frac{\partial\pi_z}{\partial z}\right),\\
H_x &= -(\sigma+i\omega\varepsilon)\frac{\partial\pi_z}{\partial y},\\
E_y &= \frac{\partial}{\partial y}\left(\frac{\partial\pi_x}{\partial x} + \frac{\partial\pi_z}{\partial z}\right),\\
H_y &= -(\sigma+i\omega\varepsilon)\left(\frac{\partial\pi_x}{\partial z} - \frac{\partial\pi_z}{\partial x}\right),\\
E_z &= -i\omega\mu(\sigma+i\omega\varepsilon)\pi_z + \frac{\partial}{\partial z}\left(\frac{\partial\pi_x}{\partial x} + \frac{\partial\pi_z}{\partial z}\right),\\
H_z &= (\sigma+i\omega\varepsilon)\frac{\partial\pi_x}{\partial y}.
\end{aligned} \tag{8}$$

The Hertz vector components π_x and π_z are the solutions of the wave equations

$$\nabla^2 \pi_{x_j} = \gamma_j^2 \, \pi_{x_j}, \tag{9}$$

and

$$\nabla^2 \pi_{z_j} = \gamma_j^2 \, \pi_{z_j}, \tag{10}$$

The solution of these wave eqs. (9) and (10) for the air (π_o), the homogeneous layers (π_j), and the lower half-space (π_N) of the model with constant radiation constants can be written directly as

$$\pi_{x_0} = M \int_0^\infty \frac{\lambda}{n_0} e^{-n_0|z-h|} \, J_0(\lambda \rho) d\lambda + \int_0^\infty A(\lambda) e^{-n_0 z} \, J_0(\lambda \rho) d\lambda, \tag{11}$$

$$\pi_{x_j} = \int_0^\infty \left\{ B_{j_1}(\lambda) e^{-n_j z} + B_{j_2}(\lambda) e^{-n_j z} \right\} J_0(\lambda \rho) d\lambda, \quad \text{for } j = 1,2,3,\ldots,\ j-1,\ j+1,\ldots,\ N-1, \tag{12}$$

$$\pi_{x_N} = \int_0^\infty D(\lambda) e^{n_N z} J_0(\lambda \rho) d\lambda, \tag{13}$$

and

$$\pi_{z_0} = \frac{\partial}{\partial x} \int_0^\infty Z_0 \, J_0(\lambda \rho) d\lambda = -\cos\phi \int_0^\infty Z_0 \, \lambda \, J_1(\lambda \rho) d\lambda, \tag{14}$$

$$\pi_{z_j} = \frac{\partial}{\partial x} \int_0^\infty Z_j \, J_0(\lambda \rho) d\lambda = -\cos\phi \int_0^\infty Z_j \, \lambda \, J_1(\lambda \rho) d\lambda, \quad \text{for } j = 1,2,\ldots,\ j-1,\ j+1,\ldots,\ N-1, \tag{15}$$

$$\pi_{z_N} = \frac{\partial}{\partial x} \int_0^\infty Z_N \, J_0(\lambda \rho) d\lambda = -\cos\phi \int_0^\infty Z_N \, \lambda \, J_1(\lambda \rho) d\lambda, \tag{16}$$

where

$$Z_0 = P_0(\lambda) e^{-n_0 z}, \tag{17}$$

$$Z_j = P_{j_1}(\lambda) e^{-n_j z} + P_{j_2}(\lambda) e^{-n_j z}, \quad \text{for } j = 1,2,\ldots,\ j-1,\ j+1,\ldots,\ N-1, \tag{18}$$

$$Z_N = P_N \, e^{n_N z}, \tag{19}$$

with $\gamma_i = \sqrt{i\omega\mu_j\sigma_j}$ and $n_j = \sqrt{\lambda^2 + \gamma_j^2}$, for all j.

The solution of the wave eqns. (9) and (10) for the transition layer has been obtained which gives the Hertz vector potential π_x and π_z in the transition layer as

$$\pi_x(z) = \int_0^\infty t^{1/2} \left[C_1(\lambda) \, J_{1/3}\left(2/3 \, t^{3/2}\right) + C_2(\lambda) \, J_{-1/3}\left(2/3 \, t^{3/2}\right) \right] J_0(\lambda \rho) d\lambda. \tag{20}$$

and

$$\pi_z(z) = \frac{\partial}{\partial x} \int_0^\infty t^{1/2} \left[Q_1(\lambda) \, J_{1/3}\left(2/3 \, t^{3/2}\right) + Q_2(\lambda) J_{-1/3}\left(2/3 \, t^{3/2}\right) \right] J_0(\lambda \rho) d\lambda. \tag{21}$$

After obtaining the solution of the wave eqs. (9) and (10) for different layers, the appropriate boundary conditions requiring the continuity of the tangential electric and magnetic fields were utilised to derive the field components over the surface of the proposed model. These boun-

dary conditions in general for the interface lying between j-th and (j+1)-th layer are

$$\gamma_j^2 \, \pi_{x_j} = \gamma_{j+1}^2 \, \pi_{x_{j+1}}, \tag{22}$$

$$\gamma_j^2 \frac{\partial \pi_{x_j}}{\partial z} = \gamma_{j+1}^2 \frac{\partial \pi_{x_{j+1}}}{\partial z}, \tag{23}$$

$$\gamma_j^2 \, \pi_{z_j} = \gamma_{j+1}^2 \, \pi_{z_{j+1}}, \tag{24}$$

$$\left(\frac{\partial \pi_{x_j}}{\partial x} + \frac{\partial \pi_{z_j}}{\partial z} \right) = \left(\frac{\partial \pi_{x_{j+1}}}{\partial x} + \frac{\partial \pi_{z_{j+1}}}{\partial z} \right), \tag{25}$$

The constants $A(\lambda)$, $B_{i_1}(\lambda)$, $B_2(\lambda)$ for all $i \neq j$, $C_1(\lambda)$, $C_2(\lambda)$ and $D(\lambda)$ are evaluated using the boundary conditions given by eqs. (22) and (23), at different interfaces. The application of these boundary conditions at N interfaces gives rise to a system of $2N$ linear equations, with the help of which one has to find the value of $2N$ unknowns. Similarly, the constants $P_o(\lambda)$, $P_{i_1}(\lambda)$, $P_{i_2}(\lambda)$, for all $i \neq j$, $Q_1(\lambda)$, $Q_2(\lambda)$ and $P_N(\lambda)$ are evaluated using the boundary conditions given by eqs. (22) through (25). The application of these boundary conditions also gives rise to another system of $2N$ linear equations. The solution of these systems of equations would give the values of constants for a general N-layer model having assumed conductivities in different layers, whereafter the field components over the surface of the model with the desired number of layers can be obtained.

In the following section, the solution for the three-layer earth model with the intermediate inhomogeneous layer, having linearly varying conductivity, acting as transition zone between the top and bottom homogeneous layers is presented. For such a three-layer model, the components of the electric and magnetic fields on the surface of the model under quasi-static approximations are derived as

$$E_{x_0} = -2i\omega\mu_0 \, C \, T_5, \tag{26}$$

$$E_{y_0} = -\frac{2C}{\sigma_1} \sin\phi \, \cos\phi \left[T_6 - \frac{T_7}{\rho} \right], \tag{27}$$

$$E_{z_0} = 2i\omega\mu_0 \, C \cos\phi \, T_4, \tag{28}$$

$$H_{x_0} = 2C \sin\phi \cos\phi \left[T_1 - \frac{T_4}{\rho} \right], \tag{29}$$

$$H_{y_0} = -2C \left[T_3 + \cos^2\phi \left(T_1 - \frac{T_4}{\rho} \right) \right], \tag{30}$$

$$H_{z_0} = -2C \sin\phi \; T_2, \tag{31}$$

$$T_1 = \int_0^\infty \frac{\lambda^2}{(\lambda + n_1)} \left[\frac{1 + We^{-2n_1 h_1}}{1 + \left(\frac{\lambda - n_1}{\lambda + n_1} \right) We^{-2n_1 h_1}} \right] J_0(\lambda\rho)\, d\lambda, \tag{32}$$

$$T_2 = \int_0^\infty \frac{\lambda^2}{(\lambda + n_1)} \left[\frac{1 + We^{-2n_1 h_1}}{1 + \left(\frac{\lambda - n_1}{\lambda + n_1} \right) We^{-2n_1 h_1}} \right] J_1(\lambda\rho)\, d\lambda, \tag{33}$$

$$T_3 = \int_0^\infty \frac{\lambda n_1}{(\lambda + n_1)} \left[\frac{1 + We^{-2n_1 h_1}}{1 + \left(\frac{\lambda - n_1}{\lambda + n_1} \right) We^{-2n_1 h_1}} \right] J_0(\lambda\rho)\, d\lambda, \tag{34}$$

$$T_4 = \int_0^\infty \frac{\lambda}{(\lambda + n_1)} \left[\frac{1 + We^{-2n_1 h_1}}{1 + \left(\frac{\lambda - n_1}{\lambda + n_1} \right) We^{-2n_1 h_1}} \right] J_1(\lambda\rho)\, d\lambda, \tag{35}$$

$$T_5 = \int_0^\infty \frac{\lambda}{(\lambda + n_1)} \left[\frac{1 + We^{-2n_1 h_1}}{1 + \left(\frac{\lambda - n_1}{\lambda + n_1} \right) We^{-2n_1 h_1}} \right] J_0(\lambda\rho)\, d\lambda, \tag{36}$$

$$T_6 = \int_0^\infty \lambda^2\, J_0(\lambda\rho)\, d\lambda \tag{37}$$

and

$$T_7 = \int_0^\infty \lambda\, J_1(\lambda\rho)\, d\lambda, \tag{38}$$

$$W = \left(\frac{i + \upsilon}{i - \upsilon} \right),$$

$$\upsilon = \frac{J_{2/3}(2/3\ \xi_1) - u\, J_{-2/3}(2/3\ \xi_1)}{J_{-1/3}(2/3\ \xi_1) - u\, J_{1/3}(2/3\ \xi_1)},$$

$$u = \frac{iJ_{2/3}(2/3\ \xi_2) - J_{-1/3}(2/3\ \xi_2)}{iJ_{-2/3}(2/3\ \xi_2) + J_{1/3}(2/3\ \xi_2)},$$

$$\xi_1 = \left[\frac{in_1}{\left(\alpha_1\gamma_1^2\right)^{1/3}}\right]^3,$$

$$\xi_2 = \left[\frac{in_3}{\left(\alpha_1\gamma_1^2\right)^{1/3}}\right]^3,$$

$$\gamma_2^2(z) = \gamma_1^2\left[1 + \alpha_1(z + h_1)\right],$$

and

$$C = \frac{I\, ds}{4\pi}.$$

3. Computational scheme

Chlamtac and Abramovici (1981) have presented the solutions in terms of differential equations and used the Rung-Kutta method of numerical solution for the computational results, while in this paper the solutions for the various field components are obtained in terms of infinite-integrals containing Bessel functions of order 0 and 1, and the computations are performed using a linear digital filter algorithm.

Anderson (1979) presented a linear digital filtering algorithm, ZHANKS, for the rapid and accurate numerical evaluation of the Hankel transforms of order 0 and 1 containing complex Bessel functions. The algorithm is quite rapid and accurate in comparison to other known filters, and is based on an adaptive convolution procedure. The accuracy of the algorithm compares favorably with single-precision numerical quadrature methods for well-behaved kernels and moderate transform arguments. Therefore, for the numerical evaluation of the em response, the integral expressions T_1, T_2, T_3, T_4 and T_5 etc., occurring in the expressions of the field components, have been transformed into the corresponding Hankel transforms of order 0 and 1. Thereafter, the ZHANKS algorithm is applied to compute these Hankel transforms of order 0 and 1. As per requirement of the program, the convergence of the integrals were tested, and in the case of slow convergence or a divergent nature, they are made convergent by adding/subtracting a known integral expression with an analytic equivalent, inside the integral sign, and subsequently adjusting its equivalent outside the integral sign. As an illustration, the integral T_1 is expressed as

$$T_1 = \int_0^\infty \left[\left(1 + \frac{R_N}{R_M}\frac{n_1}{\lambda}\right)^{-1} - 0.5\right]\lambda\, J_0(\lambda\rho)\, d\lambda + 0.5\int_0^\infty \lambda\, J_0(\lambda\rho)\, d\lambda, \tag{39}$$

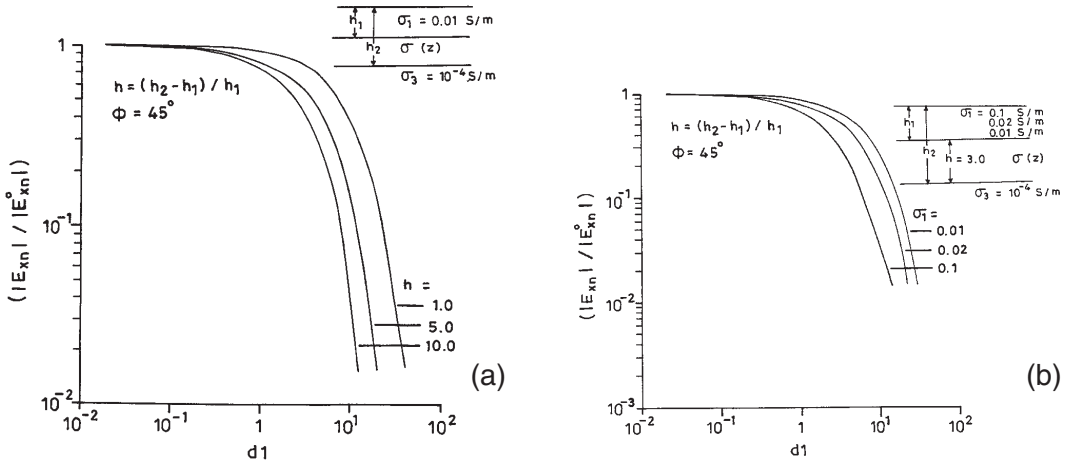

Fig. 2 - Plot of $|E_{x_n}|/|E^0_{x_n}|$ vs. d_1, showing the effect of variation of: a) transition layer thickness; b) conductivity contrast between the top and bottom layers.

with

$$R_M = 1 + We^{-2n_1h_1},$$

$$R_N = 1 - We^{-2n_1h_1},$$

and under the limiting conditions,

$$\frac{1}{1+\dfrac{R_N}{R_M}\dfrac{n_1}{\lambda}} \approx 1/2 \qquad \text{as } \lambda \to \infty$$

In equation (39), the first part is evaluated using ZHANKS, whereas the second part is directly evaluated using the relation (Watson, 1944)

$$\int_0^\infty \lambda J_0(\lambda\rho)\,d\lambda = 0. \tag{40}$$

Further, for evaluating the Bessel functions in the kernels, standard expressions were used (McLachalan, 1955).

4. Results and discussions

For studying the influence of linear variation of subsurface conductivity on em response, different three-layer earth models were chosen, with the assumption that the conductivity of the top layer gradually merges into that of the basement or substratum following the linear variation in the transition layer. The computations were performed for the absolute-amplitude ratio, the ratio of the absolute amplitude of the field component over the model, and the corresponding component over the homogeneous half space having the conductivity of the top layer of the model, of

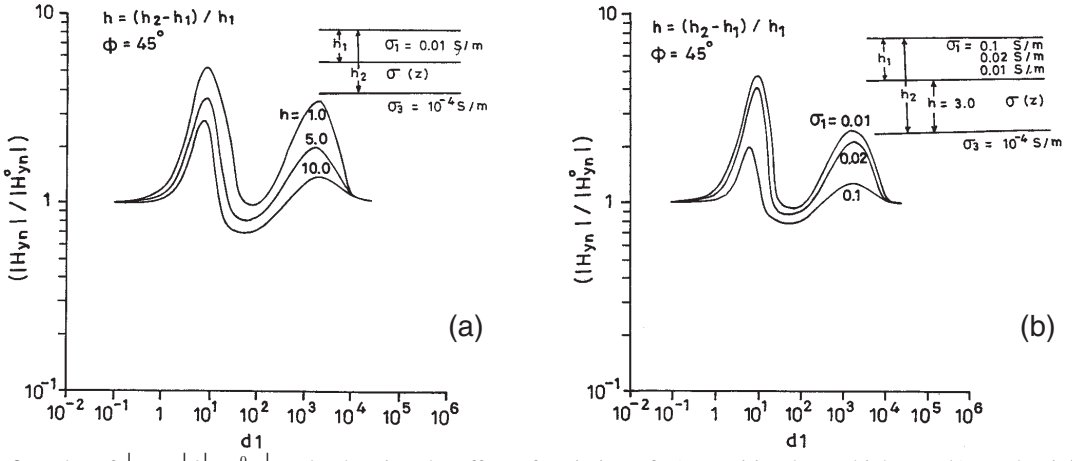

Fig. 3 - Plot of $|H_{y_n}|/|H^0_{y_n}|$ vs d_1, showing the effect of variation of: a) transition layer thickness; b) conductivity contrast between the top and bottom layers.

different field components, namely E_x, H_y and E_z; and the results showing the effect of variation of transition layer thickness and conductivity contrast between the top and bottom layers are presented as a function of numerical distance $d_1=(\omega\mu_o\sigma_1)^{1/2}\rho$. Here, ρ is the separation between transmitter and receiver, and all the other symbols are as defined earlier. It may be mentioned here that the field components for the homogeneous half-space were obtained in the computational stage by making proper substitutions.

The variation of absolute amplitude ratio of the E_x, H_y and E_z components, with numerical distance d_1, for the relative transition layer thicknesses $h = (h_2 - h_1) / h_1 = 1.0$, 5.0 and 10.0, are presented in the Figs. 2a, 3a and 4a for the model inset in the figures; and for the relative conducivity contrast between the top and bottom layers, they are shown in the Figs. 2b, 3b and 4b. A general observation of these results reveals that all the curves show their characteristic variation only for the intermediate values of numerical distance. This fact implies that the inhomogeneous model manifests its effect mainly in the intermediate range of numerical distance values. The nature of the curves are similar to those obtained by Chlamtac and Abramovici (1981).

Fig. 2a, showing the variation of absolute amplitude ratio of the E_x component with d_1, for the relative thicknesses of the transition layer depicts that these curves have a value close to unity for smaller values of d_1, and then at $d_1 \approx 0.1$, they start decreasing exponentially to attain a lower value for $d_1>10$. With increase in thickness of the transition layer, the decrease in amplitude starts at smaller values of numerical distance. The variation of the absolute amplitude ratio of the E_x component with d_1 for different conductivity contrasts, presented in Fig. 2b, shows a similar trend as in Fig. 2a. It is noticed that as the conductivity contrasts, presented in Fig. 2b, shows a similar trend as in Fig. 2a. It is noticed that, as the conductivity contrast decreases, the curves start to decrease at larger values of numerical distance and shift towards the larger values of d_1. This changing pattern may be related to the changes associated with the model.

From the Fig. 3a, showing the variation of the absolute amplitude ratio of the H_y component with d_1 for the various thicknesses of transition layer, it is observed that the curves have a value close to unity for small values of d_1. At $d_1 \approx 0.3$, they start to increase and attain a maximum peak

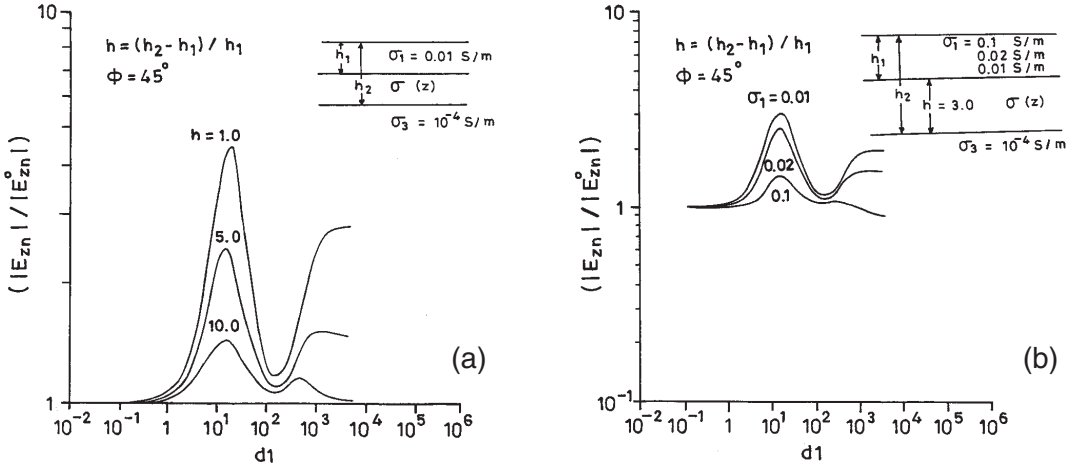

Fig. 4 - Plot of $|E_{z_n}|/|E^0_{z_n}|$ vs. d_1, showing the effect of variation of: a) transition layer thickness; b) conductivity contrast between the top and bottom layers.

at $d_1 \cong 8$, and then, decrease to attain a lower peak at $d_1 \approx 80$; they again start incrasing at $d_1 \cong 10^2$ and $d_1 \cong 10^4$. Thereafter, for $d_1 > 10^4$ the curves again maintain a value close to unity. As the thickness of transition layer increases, the maximum peak decrease in amplitude and width. From Fig. 3b, showing the effect of variation of conductivity contrast on the absolute amplitude ratio curve of the H_y component, it is seen that with decrease in the conductivity contrast, the curves show an increase in amplitude and width. This variation in the shape of the curves may be related to the model characteristics.

Fig. 4a showing the variation of the absolute amplitude ratio of the E_z component with d_1, for relative thicknesses of transition layer, reveals that for smaller value of d_1 the curves have values close to unity. At $d_1 \approx 0.3$, they start to increase and attain a maximun peak at $d_1 \approx 20$, and thereafter decrease to attain unity at ($10^2 < d_1 < 3\times10^2$). After $d_1 > 3\times10^3$, the curves again show an increasing trend. As the thickness of the transition layer increases, the maximum peak of the conductivity of the top layer, the E_z curves decrease in amplitude an width.

5. Conclusions

The present study deals with a simple and comprehensive approach of calculating the em field response of a horizontal electric dipole placed over the surface of a vertically inhomogeneous earth model having linear variation of conductivity with depth. The problem is formulated for a multi-layer earth model and the results are obtained for the representative three-layer earth models with the intermediate transition layer having the linear variation of conductivity with depth. The analytical solutions are obtained in terms of infinite integrals, and the computations are performed by using a linear digital filter algorithm, ZHANKS, in contrast to those of traditional methods involving differential equations and numerical methods of computation. The

algorithm is based on adaptive convolution theory and is acknowledged to be quite rapid and accurate. The accuracy of the algorithm compares favorably with single-precision numerical quadrature methods for well-behaved kernels and moderate transform arguments.

The computational results for the absolute amplitude ratio of the E_x, H_y and E_z components, showing the effects of variation of relative transition layer thickness and conductivity contrast, are plotted against numerical distance (d_1). A general observation of these curves reveals that all the curves are similar to those of Chlamtac and Abramovici (1981), and that they show their characteristic variation mainly in the intermediate range of numerical distance values. As the thickness of the transition layer increases, the peaks of the H_y and E_z curves decrease in amplitude and width. Further, it is also observed that with decreasing conductivity contrast, the curves manifest different variations for different components. These variations may be related to the model characteristics.

Acknowledgements. The authors wish to thank the referees for their valuable suggestions for improving this paper. One of the authors (NPS) is thankful to the Council of Scientific and Industrial Research, New Delhi, for providing the financial assistance in the form of a fellowship.

References

Abramovici F. and Chlamtac M.; 1978: *Fields of a vertical magnetic dipole over a vertically inhomogeneous earth.* Geophysics, **43**, 954-966.

Anderson W. L.; 1979: *Numerical integration of related Hankel transforms of order 0 and 1 by adaptive digital filtering.* Geophysics, **44**, 1287-1305.

Chlamtac M. and Abramovici F.; 1981: *The electromagnetic fields of a horizontal dipole over a vertically inhomogeneous and anisotropic earth.* Geophysics, **46**, 904-915.

Mallick K. and Roy A.; 1971: *Vertical magnetic dipole over transitional earth.* Geophysical prospecting, **19**, 388-394.

McLachalan N. W.; 1955: *Bessel functions for engineers.* Oxford Univ. Press, New York.

Singh N. P. and Lal T.; 1995: *Horizontal magnetic dipole over inhomogeneous earth model with exponential variation of conductivity.* Pageoph, **144**, 135-153.

Ward S. H.; 1967: *Electromagnetic theory for geophysical applications.* In: Mining Geophysics, Volume II, Theory, Soc. Expl. Geophys., 13-196.

Watson G. N.; 1944: *Theory of Bessel functions.* Cambridge Univ., press, London, pp. 386.